

CARMA Memorandum Series #16

Hybrid Star/Optimal CARMA Configurations for
Cedar Flats

Glen R. Petitpas

University of Maryland

College Park MD, USA 20742

petitpas@astro.umd.edu

September 29, 2003

ABSTRACT

I present results from my attempt to nest 5-arm star C and D arrays in between the *existing* A,B and E arrays of Helfer (2003) for the purpose of simplifying the required road and cable trenches for the more compact arrays. We have generated C and D arrays that uses the existing A,B and E array pads, and places the other pads needed for C and D arrays within the confines of a 5-arm star with arms of width 10 metres. The beam properties are respectable, but the overall result is that there are too many constrained parameters for our beams to be competitive unless the cost savings are significant. These configurations save money by populating the entire set of 5 configuration with just 51 antenna pads and may significantly simplify the road and cable trenching requirements in the inner few hundred metres. The savings need to be assessed in more detail.

1. Introduction

The Boone (2001) code is an excellent tool for generating arrays with acceptable beam properties and good UV coverage. It does have some major drawbacks. The first is that it lays antennas anywhere it needs. The optimized configurations of Helfer (2003) yield excellent uv -coverage and beams with good resolution and sidelobe properties. Since there are no spatial constraints placed on where dishes are placed, the resulting configurations are difficult to connect with roads and cable trenching will need to be solid enough to allow the transporter to drive over them while fully loaded.

The purely star arrays of Petitpas & Mundy (2003) produce a nearly equally well behaved set of array configurations while keeping all antennas (except a few A arrays ones) constrained within the arms of a 5-arm star. These configurations offer good savings in road and cable trenching costs, but will need fine tuning to fit into the surrounding geography.

It was suggested that to alleviate some of the confusion of cable trenching and transporter navigation I attempt to design an array that is configured in a 5-arm star pattern for the compact configurations (C, D, and E) while keeping the A and B arrays of Helfer (2003) intact. The benefit is that star shaped C and D arrays will simplify road and cable construction in the more crowded part of the array, while leaving the optimized A and B arrays and well thought out compact E arrays intact.

The arrays presented below are an attempt at a combination of the best parts of the arrays of Helfer (2003) with the ease of construction of the arrays of Petitpas & Mundy (2003).

2. The Configurations

We have modified the existing site “mask” used by Helfer & Wright (2003) to overlay a five arm star with arms of width 10 m (see Figure 1). I moved the centre of the star mask until the existing B array pads were as near the arms of the star as possible. We are still using the Boone (2001) optimization code, but now with much stronger spatial constraints.

Since I was attempting to achieve a C array with a resolution of $0.9''$ (at 230 GHz) resolution I locked all existing B and A array pads from Helfer (2003) within 375 m of the array centre into place. The remaining eight dishes were allowed to move freely into optimized locations within the star shaped mask.

Using this C array, I then locked the seven pads within the inner 150 m into place, and let the remaining eight dishes move to the optimal location for an array with a target resolution of $2.2''$. The resulting D array barely resembles a 5-arm star, but all pads are still technically within 10 metres of the five main arms.

The final step was to print the freshly generated D array and the E array of Helfer (2003) with the same scales onto transparencies and translated N-S and E-W until the maximum number of pads

could be reused between arrays. Using this primitive technique, we can reuse 5 pads between the D and E arrays, and no strong constraints were placed on the optimization of the D array.

Our arrays are shown in Figure 2. The resulting beams are shown in Figure 3. For completeness our uv coverage and uv density vs baseline plots are shown in Figures 4 and 5 respectively.

3. Results

Our beams are shown in Figures 3. The contour levels are -10, -5, 5, 10, 20, 40, 60, 80, 100%. Details of the beams and sidelobes are presented in Table 1. The sidelobe information in Table 1 is for the inner 14×14 beams only. The sidelobe statistics for a larger area of 40×40 beams is presented in Table 2.

Considering the strong constraints placed on the optimization of these two arrays, the resulting beams are not too different from the purely optimized arrays of Helfer (2003) and the pure star arrays of Petitpas & Mundy (2003).

The difference in the beam sizes between adjacent array is typically 2.5 as desired (see Table 3). The exception is the D and E arrays.

4. Assessment

While the beam properties are respectable given the strong constraints we placed on the pad locations and forced pad reuse, we feel that they are not as good overall as the purely optimized arrays of Helfer & Wright (2003) and Helfer (2003) or the purely star arrays of Petitpas & Mundy (2003).

Given that we are forced into the star shape *after* the optimal placement of the A and B arrays of Helfer & Wright (2003) the main driver of the star array has already been lost; namely, the placement of all pads along narrow roads. By the time you get to C and D arrays configurations, the 10 metre wide arms of the star are a significant fraction of the radius of the arms, and you are simply left with a vaguely star-like shape, with little to be saved on pad reuse and road/cable construction. Roads will still need to be run in addition to the 5 arms to reach the A and B array pads of Helfer (2003).

We cannot assess what sort of simplification this hybrid star-optimal array will create.

We note that this set of configurations offers an impressive improvement in pad reuse over the purely optimized arrays of Helfer (2003). In re-doing only the C and D arrays, we were able to do away with a surprising 10 pads. We need 51 pads to populate these arrays, whereas Helfer (2003) require 60 pads.

5. Summary

1) We have generated a series of C and D array configurations that have respectable beam properties and superb pad reusage.

2) Can cannot assess what sort of savings and simplification in construction and operation these hybrid configurations will generate, but it would likely have to be significant in order to justify the use of these configurations over the purely star arrays of Petitpas & Mundy (2003) or purely optimal arrays of Helfer & Wright (2003).

3) We do note that despite only being allowed to modify two out of the five arrays, we were still able to reduce the number of pads needed to populate all five arrays by 9 (or an overall reduction in pads of 15%).

G. R. P. is supported by NSF grant AST 99-81289 and by the State of Maryland via support of the Laboratory for Millimeter-Wave Astronomy.

REFERENCES

Boone, F., 2001, *A&A*, 377, 368

Helfer, T., & Wright, M., 2003, CARMA Memo, *in prep.*

Helfer, T., 2003, CARMA Memo, *in prep.*

Petitpas, G. R., & Mundy, L. G., 2003, CARMA Memo, *in prep.*

Table 1. Beam Parameters for the 5-Arm Star Arrays at 230 GHz

Cfg	δ ($^{\circ}$)	HA,inc (hrs)	σ (mJy)	$\theta_{\max} \times \theta_{\min}$ ($''$)	σ_{T_b} mK	SL rms (%)	max (%)	min (%)	Nvis (%)	uv min (m)	uv max (m)
C	30	-2,2,.01	0.23	0.93 x 0.70	8.2	2.8	11.8	-6.3	100	25.8	391.8
C	0	-2,2,.01	0.27	1.01 x 0.81	7.6	3.0	12.3	-7.1	100	20.4	390.6
C	-30	-2,2,.01	0.57	2.91 x 0.90	7.5	2.6	8.7	-6.5	100	8.7	363.9
D	30	-2,2,.01	0.23	2.26 x 2.05	1.1	2.5	7.8	-6.2	100	11.7	138.0
D	0	-2,2,.01	0.27	2.60 x 2.24	1.1	2.9	12.7	-6.9	100	8.7	132.3
D	-30	-2,2,.01	0.68	4.43 x 1.93	2.0	4.2	11.3	-8.5	58	4.2	120.6

Beam properties for the 5-arm star arrays shown in Figure 2. Column (1) is the array configuration; column (2) is the declination; column (3) is the LST range and step size of the observations; column (4) is the sensitivity (in mJy); column (5) beam size (in $''$); column (6) is the brightness temperature sensitivity (in mK). Columns (7),(8), and (9) are the sidelobe rms, max and min (respectively) over a $\sim 14 \times 14$ beam area. Column (10) is the percentage of unshadowed visibilities while columns (11) and (12) projected minimum and maximum baselines (in meters).

Table 2. Comparison of Sidelobe Parameters over $\sim 40 \times 40$ Beams for the 5 Arm Star and Helfer & Wright (2003)

dec	Array	rms	max	min	Array	rms	max	min
30	star C	2.2	13.1	-6.3	opt C	2.2	8.4	-5.9
0		2.8	15.0	-7.1		2.9	27.6	-6.9
-30		2.3	8.7	-6.5		2.2	7.9	-6.2
30	star D	2.3	10.2	-6.4	opt D	2.2	9.8	-6.1
0		3.2	35.6	-7.0		3.1	28.8	-7.1
-30		2.8	11.3	-8.5		2.2	8.3	-6.4

Direct comparison of the sidelobe properties between the 5 Arm star (left columns) and those of Helfer & Wright (2003) (labelled “opt C and D” in the right columns). We note that the maximum sidelobe is not a very robust measure of beam quality, and changes significantly with the removal of antennas from the array or variations in LST range over which the observations are taken. The “rms” sidelobe is more robust to small changes in observing parameters.

Table 3. Beam elongations, spatial dynamics ranges and SRFs at $\delta = 30^\circ$

Config	θ_{\max} (")	θ_{\min} (")	$\theta_{\max}/\theta_{\min}$	S_{\max}/S_{\min}	SRF
opt B	0.37	0.30	1.23	11.6	
star C	0.93	0.70	1.33	15.2	C/B = 2.4
star D	2.26	2.05	1.10	11.8	D/C = 2.6
opt E	4.48	3.94	1.14	8.8	E/D = 2.0

Array beams and scale factors for the C and D 5 arm star array combined with the optimized B and E arrays of Helfer (2003). Column (1) is the array; columns (2) and (3) are the maximum and minimum beam elongation and column (4) is the ratio of the two. Column (5) is the ratio of maximum to minimum projected baseline and the last column is the Scale Resolution Factor between the average beam elongation of subsequent arrays.

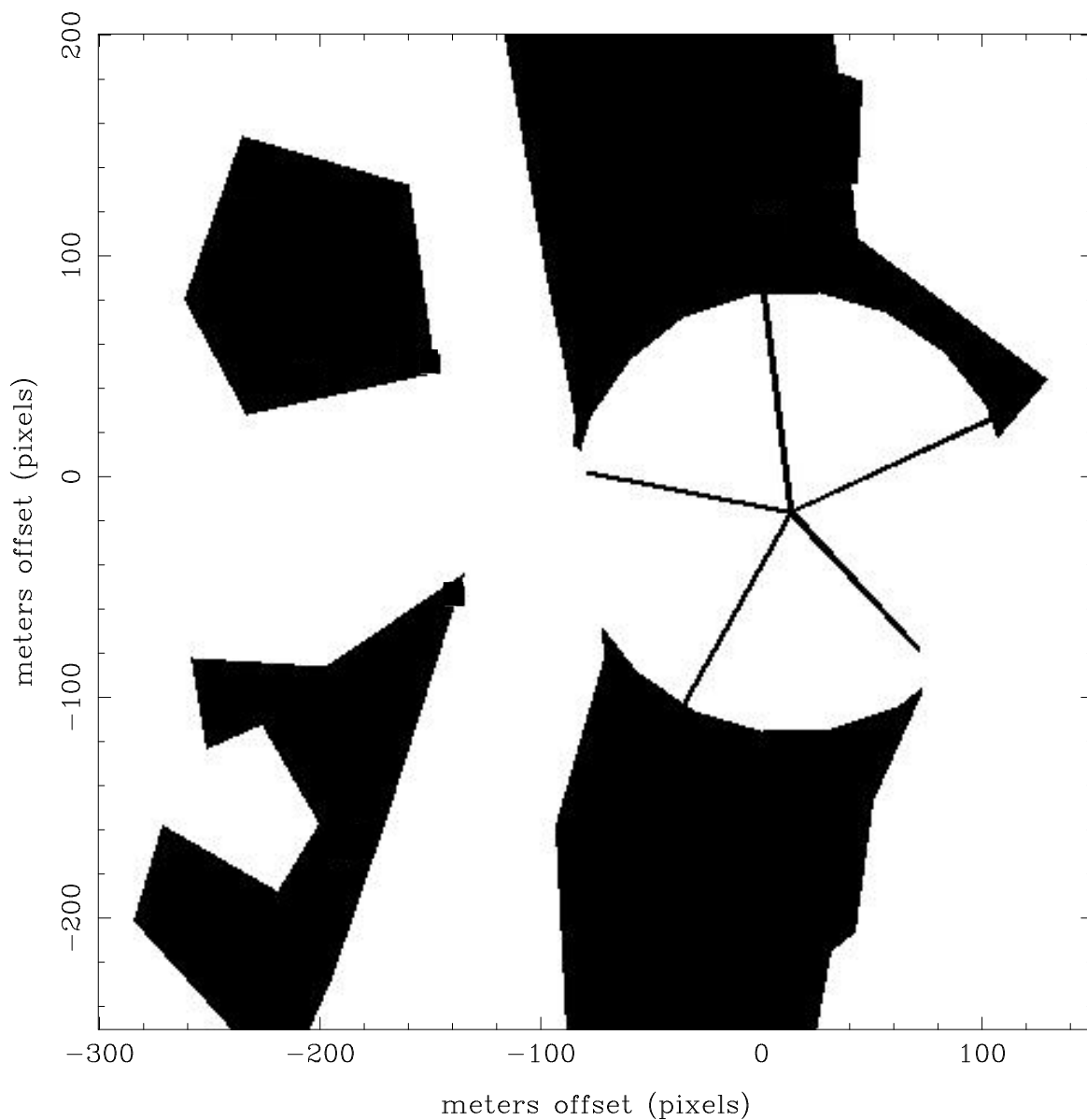


Fig. 1.— Shown is the mask used to generate the configurations shown in Fig 2. The arms are 500 m in radius and 10 m wide. The star orientation was chosen so that the large hill to the NE of the array center is between two arms. Also, it was important to try and keep only one arm crossing the ridge to the west of the array center (between the center and Rt 168).

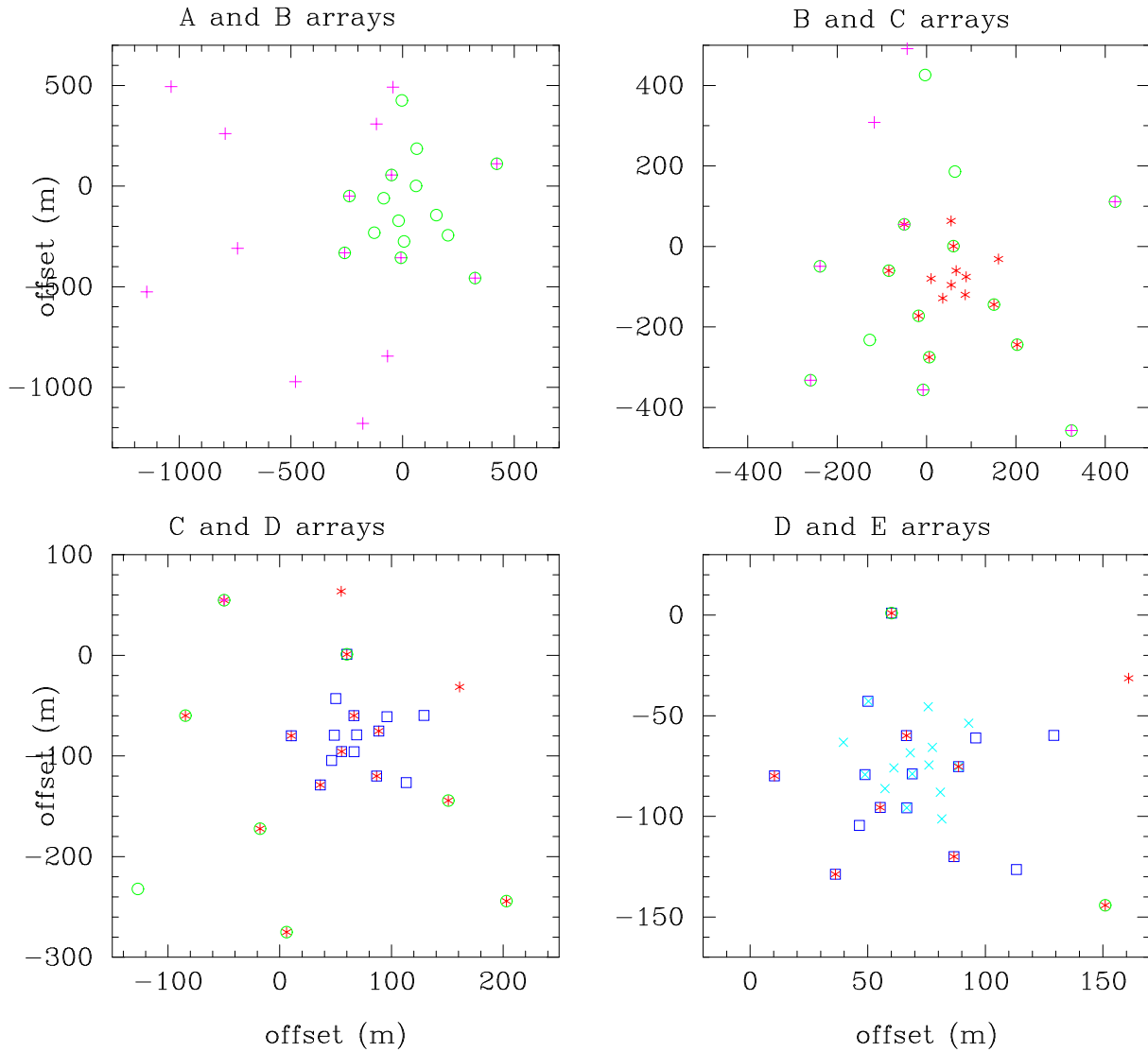


Fig. 2.— We zoom in on the arrays. The purple +’s mark the A array pads, the green circles mark the B array pads, the red *’s mark the C array pads, the blue squares mark the D array pads and the turquoise ×’s mark the E array pads. It is most likely that we will incorporate the superior E array of Helfer & Wright in place of our E-array. In this case we will need to add 3 more pads.

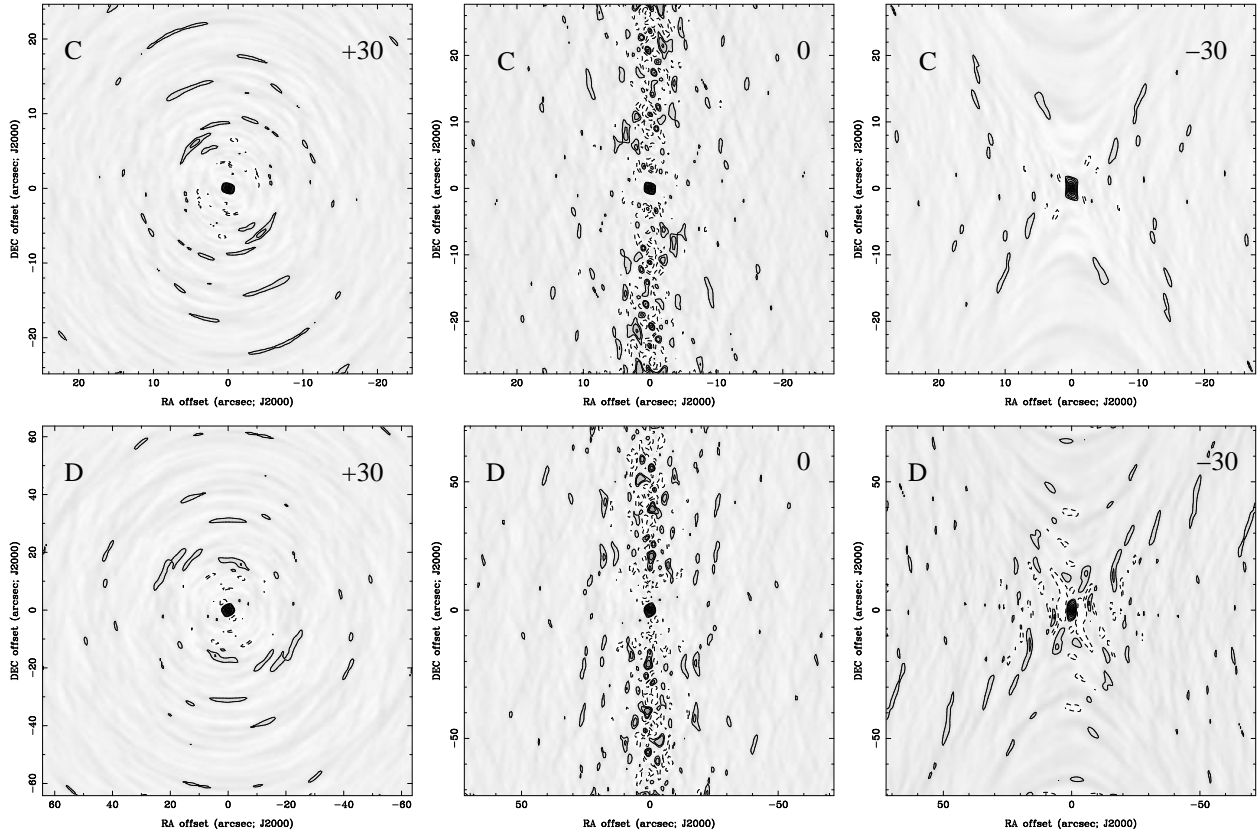


Fig. 3.— The resulting beams for the configurations shown in Figure 2. From top to bottom are the C and D arrays respectively. From left to right we show beams for declinations of +30, 0, and -30 (respectively). The contour levels are -0.1, -0.05, 0.05, 0.1, 0.2, 0.4, 0.6, 0.8, 1.0 (fractions of the peak).

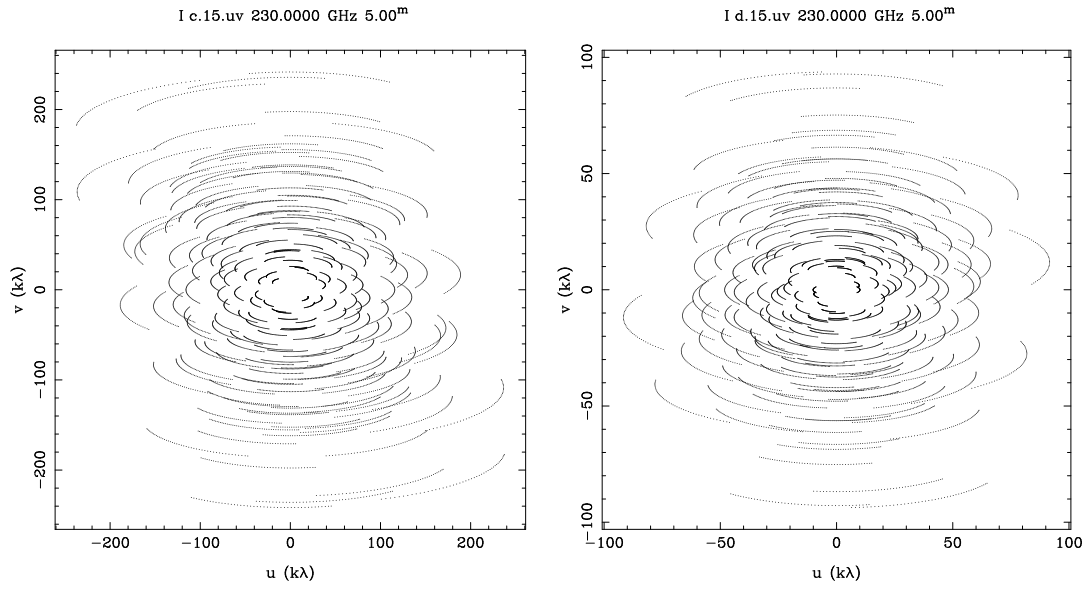


Fig. 4.— uv plots for each of the C (top) and D (bottom) configurations at a declination of $+15^\circ$.

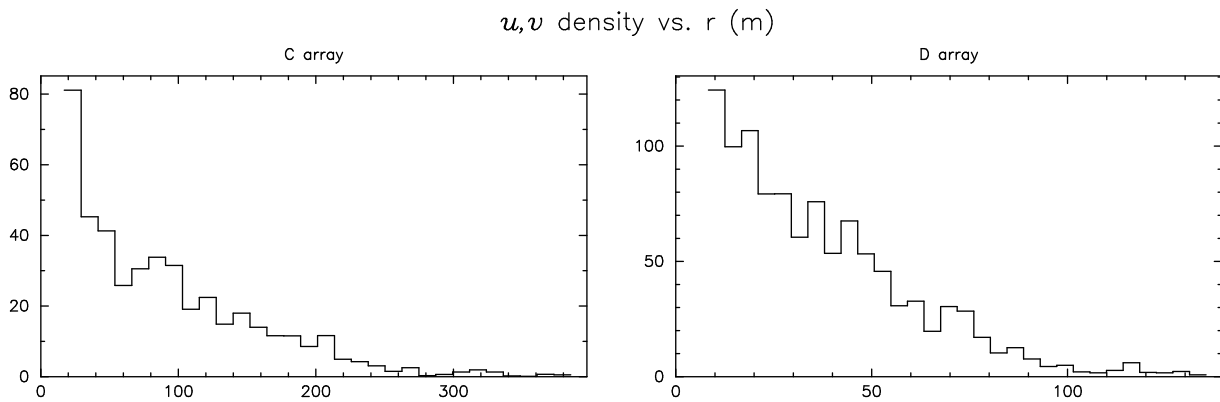


Fig. 5.— uv density plots for each array showing the Gaussian distribution generated by the Boone code. What is not taken into account is the fact that the larger OVRO will weight some of these baselines differently, resulting in a slightly different (and perhaps non-optimal!) distribution than is shown here.